Methodological guidelines to isolate and purify plant extracellular vesicles

Determining the correct approach of isolating and purifying plant extracellular vesicles

Yifan Huang[1], Shumei Wang[2], Qiang Cai[1,3]* and Hailing Jin[2]*

[1]State Key Laboratory of Hybrid Rice, College of Life Science, Wuhan University, Wuhan, 430072, China;

[2]Department of Microbiology and Plant Pathology and Center for Plant Cell Biology, Institute for Integrative Genome Biology, University of California, Riverside, California 92507, USA;

[3]Hubei Hongshan Laboratory, Wuhan, 430072, China.

*Correspondences: Qiang Cai (qiang.cai@whu.edu.cn); Hailing Jin (hailingj@ucr.edu)

ABSTRACT

Plant extracellular vesicles (EVs) have become the focus of rising interest because of their important roles in cross-kingdom trafficking molecules from hosts to interacting microbes to modulate pathogen virulence. However, the isolation of EVs from plants still represents a considerable challenge. Currently, plant EVs have been isolated from apoplastic washing fluid (AWF) using a variety of isolation methods. In this study, using the *Arabidospsis* as a model, we detailed described the ideal method for AWF collection, and following EV isolation based on differential ultracentrifugation. Among two commonly speed, 40,000 × g and 100,000 × g, used in plant EV final ultracentrifugation, centrifuge at 100,000 × g is the better option. Methods for EV further separation from heterogeneous vesicles, including iodixanol density-based separation and immunoaffinity capture were also described. We showed that the use of immunoaffinity capture provided significant advantages for plant EV isolation when antibody and suitability of EV markers available. Overall, this study should serve as a

guide to choose and further optimize EV isolation methods for their desired downstream applications.

INTRODUCTION

Cell-to-cell communication between plants and pathogens requires secretion, and delivery of molecular signals into extracellular environment and transporting into interacting organisms, which is essential for both plants and pathogens survival (Kimura et al. 2001; Mahlapuu et al. 2016; Toruno et al. 2016). Recent research has demonstrated that RNAs, including regulatory small RNAs (sRNAs), are able to move between pathogens and their hosts and regulate biological process in recipient cells (Knip et al. 2014; Zhang et al. 2016b; Cai et al. 2018; Cai et al. 2019b; Huang et al. 2019). It was a long time unclear the mechanisms used to pass these sRNAs through multiple barriers and into the opposing host or fungal cells. The recently studies showed that extracellular vesicles (EVs) are the vehicles that carry sRNAs across kingdoms trafficking from plants to pathogens (Cai et al. 2018; Hou et al. 2019). Currently, plant EVs have attracted a big deal of interest because of their numerous functions in bioactive molecules exchange and cell-to-cell communication (Mathieu et al. 2019; Cai et al. 2021; Kameli et al. 2021).

EVs are small, lipid bilayer-enclosed vesicles containing transmembrane proteins, enclosing soluble proteins and RNAs, that can be released by cells from different organisms, including eukaryotes and prokaryotic cells (Colombo et al. 2014; van Niel et al. 2018). EVs are heterogeneous groups of vesicles with different sizes and intracellular origin, comprising exosomes, microvesicles and apoptotic bodies, which originate from the multivesicular bodies (MVBs), shed from the plasma membrane, and apoptotic cell during apoptosis, respectively (Akers et al. 2013; Colombo et al. 2014; van Niel et al. 2018). In plant, EVs has been initially observed in carrot cell cultures by transmission electron microscopy (TEM) in 1967 (Halperin and Jensen 1967). Since then, plant EVs were observed to enriched in fungus-plants interaction sites by TEM, such as *Blumeria graminis f. sp.hordei* infected barley epidermal cells (An et al. 2006a;

An et al. 2006b), *Botrytis cinerea* infected *Arabidopsis* leaf cells (Cai et al. 2018), and *Rhizophagus irregularis* arbuscules in rice root (Roth et al. 2019). TEM and confocal microscopy analysis demonstrated plant MVBs fused with the plasma membrane underlying fungal or oomycete invasion sites, which suggested that plant exosomes are released by MVB mediated secretion (An et al. 2006a; An et al. 2006b; An et al. 2007; Nielsen et al. 2012; Bozkurt et al. 2014; Cai et al. 2018).

It is worth noting that plant EVs are nanovesicles derived primarily from the apoplastic space (AWF). However, nanovesicles isolated from disrupted whole leaf tissue are not pure EVs, that mixed with disrupted intercellular membranes (Liu et al. 2020). Currently, there are few reports of EVs isolated from AWF of plant tissues: *Arabidopsis* leaves (Rutter and Innes 2017; Cai et al. 2018; He et al. 2021), sunflower seeds and seedlings (Regente et al. 2009; Regente et al. 2017), olive pollen tubes (Prado et al. 2014) and *Nicotiana benthamiana* leaves (Movahed et al. 2019). In *Arabidopsis* leaves, to our knowledge, at least three known EV subtypes exist: Tetraspanin (TET) 8 positive EVs derived from MVBs and can be considered bona fide plant exosomes (Cai et al. 2018; Cai et al. 2021), Penetration 1 (PEN1) positive EVs (Rutter and Innes 2017), and the EVs produced by EXPO that fusion with the plasma membrane (Wang et al. 2010; Ding et al. 2014). It has been demonstrated that plant endogenous sRNAs secreted by EVs as a defense mechanism against fungal pathogen (Cai et al. 2018). The further study showed TET8 positive exosomes are the major class of plant EVs that transport sRNAs, and several RNA binding proteins contribute to sRNA selective loading and stabilization in EVs (He et al. 2021).

In animals, many isolation methods for EVs have been developed in the last decade. Among them, differential ultracentrifugation separation considered as the classical standard for EV isolation, specifically for the isolation of small EVs or exosomes (Thery et al. 2006; Mathivanan et al. 2012). This method has several substeps, including centrifugation at 300 ×g to sediment cells, at 2000 ×g to remove dead cells and apoptotic bodies (large vesicles), at 10,000-15,000 ×g to remove cell debris and microvesicles (medium vesicles), and the final supernatant then ultracentrifuged at ⩾

100,000 ×g (100,000 to 200,000 ×g) to pellet general small EVs and exosomes (Thery et al. 2006; Crescitelli et al. 2013; Konoshenko et al. 2018; Willms et al. 2018; Jeppesen et al. 2019). Next, EV pellet was washed to remove non-EV proteins by resuspension and following ultracentrifugation (Thery et al. 2006; Konoshenko et al. 2018). Pellet of differential ultracentrifugation can be additional separated by extra steps, such as high-speed density gradient ultracentrifugation or bead-based immunoaffinity capture, which lead to the isolation of subtypes of EVs and increase purity of isolated EVs (Thery et al. 2006; Jeppesen et al. 2019).

While animal EVs have been well studied over the last years, plant EVs have remained poorly investigated. This is mainly due to lack of accepted EV isolation protocols. Since plant EVs derived primarily from the apoplastic space, the crucial first step is isolation of AWF, which obtained by a simple well-established infiltration-centrifugation method (Wang et al. 2005; Sanmartin et al. 2007; Hatsugai et al. 2009; O'Leary et al. 2014). Based on established animal EV separation protocols, plant EV separation involves differential ultracentrifugation of AWF, with two consecutive steps of low speed centrifugations at 2,000 ×g and 10,000 ×g to remove dead cells, cell debris and large vesicles, and high speed centrifugation at 100,000 × g to pellet the small EVs (Prado et al. 2014; Cai et al. 2018; Movahed et al. 2019; Liu et al. 2020; He et al. 2021). In some studies, the lower centrifugal force, 40,000 ×g was used for final pellet EV fractions, including PEN1-positive EVs in *Arabidopsis* (Rutter and Innes 2017) and EVs derived from sunflower seeds and seedlings (Regente et al. 2009; Regente et al. 2017). Note that different protocols for plant EV isolation differ not only in the conditions of centrifugation in final EV sedimentation but also in collection of AWF. So far, there is still no unified protocol for plant EV isolation, when assaying AWF collected from different plants. Thus, in this study, we propose the standardization of methods for plant EV isolation and separation, by using *Arabidopsis* as a model. We described gold standard for plant EV isolation in detail, and compared different differential ultracentrifugation protocols for EV isolation in the number of steps. We performed high-speed density gradient ultracentrifugation that enables EVs floated in an iodixanol gradient to separation and purification of different plant EV subtypes with

different densities. Furthermore, we also described recent developed the immunoaffinity capture method, using bead-based antibody that recognize the plant EV enriched TET8 protein, allowing the precise capture of specific TET8-positive EV subtype.

RESULTS

Isolation of plant EVs by differential ultracentrifugation

Differential ultracentrifugation is the most commonly method used for EV isolation from cell culture supernatants and biological fluids, which detailed protocol was published by Théry *et al*. in 2006 (Thery et al. 2006; Willms et al. 2018). Plant EV isolation methods share similarities with that used for mammalian EVs, except for the initial step, collecting AWF from leaves (Figure 1). Due to infiltration-centrifugation method is a well-established technique for AWF collection of various plant species, we developed a protocol for AWF extraction from *Arabidopsis* leaves (optimized vacuum infiltration and centrifugation method) (O'Leary et al. 2014; Cai et al. 2018; He et al. 2021). In this protocol, fully expanded rosette leaves were detached from plant at the petiole using a razor blade to remove phloem stream that contains large amounts of mobile RNAs and ribonucleoprotein complexes (Zhang et al. 2009; Liu and Chen 2018). Before infiltration with the buffer, cytoplasmic contaminants that exude from damaged cells were removed by washing the cut leaves in distilled water (Figure 1A). After clean leaves infiltrated with the buffer by negative pressure within a needleless syringe, apoplast washing fluid can be recovered by centrifugation at 900 ×g (Figure 1A). EVs can be settled out of AWF by ultracentrifugation that comprises five steps (Figure 1B): (i) The AWF was centrifuged for 30 min at 4 °C at 2,000 × g to remove large cell debris. (ii) The supernatants filtered by a 0.45 μm filter to further effectively remove large vesicles. (iii) The supernatant was moved into new ultracentrifuge tubes, and large vesicles were removed with another centrifugation step at 10,000 × g for 30 minutes at 4°C. We named the supernatants of this step as clean AWF. (iv) Plant EV fraction can then be pelleted under very high speed (100,000 × g) centrifugation for 1 hour. (v) A second round of ultracentrifugation at 100,000 × g for 1 hour to wash the EVs. Co-

sedimentation contaminating proteins can be removed at this step. The EV pellet of this step was named as P100 fraction.

Technical evaluation of apoplastic washing fluid (AWF) collection from *Arabidopsis* leaves

Extraction of AWF is the crucial step for EV isolation in plant. The method of this step should be taken into account when using the ultracentrifugation protocol in order to obtain less contaminated EVs. Besides detached leaves method (Figure 1A, Method 1), whole rosettes method (Method 2) (Figure S1) also be used for AWF collection prior to plant EV isolation (Rutter and Innes 2017; Baldrich et al. 2019). In Method 2, whole rosettes were harvested at root by using scissors and then vacuumed and centrifuged to collect the AWF (Figure S1). Here we compared the Method 1 along with the Method 2 for purity and quality of EVs. Because we previously showed that fungal infection increases EV secretion (Cai et al. 2018; He et al. 2021), in this study, we used *B. cinerea*-infected *Arabidopsis* to increase the yield of isolated EVs. Ideally, AWF should be free of contamination by cytoplasmic proteins such as Rubisco (O'Leary et al. 2014). However, AWF extracted by Method 2 showed much darker green than extracted by Method 1 (Figure 2A). Detected Rubisco protein by western blot provided a further quality assay of AWF samples. The presence of obviously Rubisco protein band in the AWF sample extracted by method 2, indicating it contains a greater amount of Rubisco contamination that of AWF extracted by Method 1 (Figure 2B). Furthermore, Rubisco protein band can be easy detected in the P100 sample derived from AWF extracted by Method 2 (Figure 2B). We then directly visualized the vesicles in the P100 fractions prepared from AWF extracted by Method 1 and Method 2, using transmission electron microscopy (TEM). The TEM micrographs showed P100 from Method 2 with not clean background due to non-vesicle material impurities; while no such structures were observed in P100 from by Method 1 (Figure 2C). These results support the suggestion that detached leaves method more suitable be used for AWF collection to avoid contamination.

Technical evaluation of final ultracentrifuge speed for plant isolation

In differential ultracentrifuge steps, final supernatant is finally ultracentrifuged to pellet the EVs. In animal system, as genuine exosomes (or small EVs in general) are usually sedimented at speeds north of 100,000-200,000 × g (Thery et al. 2006; Kowal et al. 2016; Konoshenko et al. 2018; Jeppesen et al. 2019). For plant EV isolation, two final ultracentrifuge speed, 100,000 × g (Prado et al. 2014; Prado et al. 2015; Cai et al. 2018; He et al. 2021; Kameli et al. 2021) and 40,000 × g (Regente et al. 2009; Rutter and Innes 2017; Baldrich et al. 2019), were used in different studies. Here we compared the final ultracentrifuge steps, either centrifuged clean AWF at 100,000 × g, or at 40,000 × g, to obtain two EV fractions, P100 and P40, respectively (Figure 3A). Centrifugation of the supernatant of P40 fraction at 100,000 × g to obtain P100-40 fraction (Figure 3A). Since the most widely used method for examining the morphology of EVs is negative staining and following imaging by TEM (Jung and Mun 2018), we imaged EVs in P100, P40 and P100-40 fractions those methods. EVs in P100 fraction showed their cup-shaped morphology (Figure 3B), that similar with animal EVs isolated by centrifuged at 100,000 × g (Thery et al. 2006; Jung and Mun 2018). Plant EVs are unlikely to be deformed or and broken during centrifugation (Figure 3B). Although some EVs observed in P40 fraction, a substantial amount EVs were isolated after centrifugation of the supernatant of fraction P40 at 100,000× g (P100-40) (Figure 3B). Furthermore, similar to the previous conclusion, isolation of EV fractions by using transgenic plants co-expressing TET8-GFP and mCherry-PEN1 proteins that could monitor TET8-positive and PEN1-positive EVs, showed large amount of TET8-positive EVs in P100-40 fraction (Figure 3B). Those results demonstrated that centrifuged at 100,000 × g has higher separation efficiency than centrifuged at 40,000 × g for plant EV isolation, and it results in large amounts of EVs losses when using a lower speed of centrifuge.

We also analyzed the plant EV size based on TEM imaging. The TEM micrographs of the P100 fraction showed a majority of vesicles (92.3%) with diameters ranging between 30 nm and 150 nm, and with the average diameter of 84.5 nm (Figure 4). This result demonstrated that plant EVs in P100 fraction have the similar size of one of EV subtypes termed exosomes (30 nm-150 nm in diameter) (Colombo et al. 2014; Kowal

et al. 2016; Mathieu et al. 2019). However, the vesicles in the P40 fraction were bigger than those in the P100 fraction, with the average diameter of 97.8 nm (Figure 4). The obviously different size of the vesicles in the P100-40 and P40 fractions was also apparent in TEM images (Figure 4). The average diameter of the vesicles in the P100-40 was 69.5 nm, which was the smallest vesicles in three fractions, suggesting centrifuged at 40,000 × g giving the priority to pellet larger vesicles. These results suggest that centrifuged at 100,000 × g enriches plant EVs much more efficiently than 40,000 × g.

Density gradient fractionation separates plant EVs

Although Method 1 provide reasonably pure plant EVs (Figure 2), for some applications it may require an extra purification step. Furthermore, exosomes, microvesicles and other large vesicles cosedimentation produces a mixture of particles in the P100 fraction (Konoshenko et al. 2018). Density gradient fractionation separation is a classical method used to separate vesicles according to their floatation speed and equilibrium density (Colombo et al. 2014; Kowal et al. 2016; Jeppesen et al. 2019). This strategy separates EVs using sucrose or iodixanol gradient centrifugation of EV pellets prepared by differential ultracentrifugation. For plant EV isolation, vesicles in P100 fraction floated in sucrose (He et al. 2021) or vesicles in P40 fraction floated in iodixanol (OptiPrep) gradient (Rutter and Innes 2017), facilitate the separation of subtypes of EVs. Here we used iodixanol density gradient to further separate EVs from P100 fraction and estimate their density using top-loading methods (Figure 5A). By using TET8 antibody, we identified most of TET8-positive EVs accumulate in third fraction (F3) at the density of on average 1.08 g/ml of iodixanol (Figure 5B), which similar with the density of exosomes in animal systems (1.08–1.12 g/ml) (Wubbolts et al. 2003; Iliev et al. 2018; Jeppesen et al. 2019). Notably, plant exosome marker TET8 were detectable in F3 fractions which confirms this fraction enriched in plant exosomes, which with majority of vesicles (93%) with diameters ranging between 30 nm and 150 nm, and with the average diameter of 68.9 nm (Figure 5C and 5D).

Immunoaffinity capture-based technique to isolate plant EVs

Immunoaffinity capture-based techniques is a simple and rapid method that suitable for the routine isolation and analysis of EVs (Thery et al. 2006; Kowal et al. 2016; Jeppesen et al. 2019; He et al. 2021). This technique relies on the use of an antibody to capture EVs based on the expression of the antigen on the surface of the EVs (Thery et al. 2006). Tetraspanin family such as CD81 or CD63, are ideal immuno-capture molecules since they are enriched on exosome membrane (Andreu and Yanez-Mo 2014). We performed a final separation step by immuno-isolation using beads coated with antibodies targeting plant exosome marker TET8 (Figure 6A). It is worth noting that antibodies recognized protein sequences must be expressed on surface and outside of EV. Thus, antibody that specifically recognizes the large exposed extravesicular loop, EC2 domain of TET8 has been well designed for pull-down TET8 positive EVs from P100 fraction (He et al. 2021). By using this method, TET8-positive EVs can be successfully isolated from P100 fraction, and then easily detected by confocal microscopy (Figure 6B). Specificity of the immunoaffinity capture was examined using beads coating an irrelevant antibody (IgG) (Figure 6B). Thus, this approach can be easily used for isolating subtype of marker-positive EVs in plant. By using this method, EV-enriched sRNAs and RNA binding proteins, AGO1, RH11, RH37, ANN1 and ANN2 were clearly detectable in the TET8-positive EVs (He et al. 2021). Thus, this immunoaffinity isolation is the gold method to precisely analysis cargo contents of specific EV subtype.

DISCUSSION

In recent years, plant-derived EVs have gained the interest, and research in this field has exponentially increased (Cai et al. 2021). In plant, EV definitions are nanovesicles that secreted by cells into apoplastic environment through exocytosis (Cai et al. 2019a). Although in some literatures, the nano-sized particles isolated from disrupted leaf or plant tissues by differential ultracentrifugation also named as plant EVs, they are actually artificial plant derived vesicles instead of true EVs (Zhang et al. 2016a; Kameli et al. 2021). Interestingly, these artificial vesicles have making their application in human health and disease very promising (Wang et al. 2013; Mu et al.

2014; Teng et al. 2018; Liu et al. 2020). Due to the existing of diversity separation methods and EV definitions in plant, in this study, we provided the standard method for AWF collection, and following EV isolation based on differential ultracentrifugation.

In animal systems, EVs have been isolated from diverse bodily fluids, including blood, urine, saliva, breast milk, semen or cell culture media (Colombo et al. 2014). For plant EV isolation, the first critical step is the collection of clean apoplastic fluids. Due to the small size and fragility of *Arabidopsis* leaves, collection of clean apoplastic fluids is a challenge. In this study, we firstly separated *Arabidopsis* leaves of similar size from the rosette, and collected AWF using vacuum infiltration and following low speed centrifugation (Method 1 in Figure 2). Due to phloem stream that contains large amounts of mobile RNAs and ribonucleoprotein complexes (Zhang et al. 2009; Liu and Chen 2018), this detach leaf protocol removes those irrelevant RNAs and minimize the impact on following analysis RNA content in EVs. We found that the other plant AWF collecting method, such as whole rosettes protocol (Method 2 in Figure 2), would lead to cell breakage. It may cause by those leaves not supported and squeeze with each other during centrifugation, and result in intracellular content (proteins and RNAs) released into AWF. In addition, mobile RNAs and ribonucleoprotein complexes in phloem stream also may be extracted into AWF. Therefore, AWF collected from detached leaves by Method 1 is more suitable as the first step of plant EV isolation.

Ultracentrifugation remains the most commonly used technique for EV isolation of EVs from different biofluids and cell culture supernatant. Similar with animal EV separations have overwhelmingly relied on 100,000 × g fractions, plant EVs and its RNA contents were highly enriched in the fraction collected by ultracentrifugation at 100,000 × g from AWF (Cai et al. 2018; He et al. 2021). In this study, we have characterized EVs from either the intermediate speed (40,000 × g) or high speed (100,000 × g) fractions. With consistence with previously study (He et al. 2021), We found that centrifuged at 100,000 × g has higher separation efficiency, and it results in large amounts of EVs losses when centrifuged at 40,000 × g. Vesicles in the P100-40 fraction containing TET8-positive vesicles, is smaller than vesicles in P40 fraction. Furthermore, vesicles in the P100-40 fraction with the average diameter 69.5 nm, which

was similar with the size of exosome in animal systems (Colombo et al. 2014; He et al. 2021). Thus, if the sedimentation rates are not sufficiently, centrifugation produces larger vesicles in pellet, whereas a portion small EVs remains in the supernatant. For example, although ultracentrifuging urine at 200,000 × g, 40% of the vesicular proteins are still present in the supernatant after ultracentrifuging urine at 200,000 ×g (Musante et al. 2013). However, centrifuged at lower speed, such as 40,000 × g, may be suitable for separating EV from AWF collected by Method 2, and PEN1-associated EVs are mainly collected at this speed (Rutter and Innes 2017; He et al. 2021). In this study, we observed large amount of non-vesicle material impurities in P100 fraction from AWF collected by Method 2, indicating non-vesicle material pelleted when centrifuged at higher speed. These could explain the previously observed small particles ranging from 10-17 nm in P100-40 fraction were those non-vesicle materials in AWF collected by Method 2 (Rutter and Innes 2017).

The density gradient centrifugation technique enables production of the EV fraction of higher purity and separate different EV subtypes (Konoshenko et al. 2018; Jeppesen et al. 2019). We previously showed vesicles in P100 fraction floated in sucrose density gradient, TET8-positive EVs and EV-enriched sRNAs enriched in the EV fractions at the density of 1.12-1.19 g/ml (He et al. 2021). In this study, P100 fraction were floated in iodixanol density gradient, and TET8-positive vesicles enriched in the gradient fraction of approximately on average 1.08 g/ml. The different density of TET8 positive EVs in sucrose versus iodixanol could be a result of differences in the osmotic pressure of these two gradients. This result was similar with the previously study that difference in separation of P100 pellets derived from human dendritic cells in sucrose versus iodixanol (Kowal et al. 2016). Note that PEN1 positive EVs collected at 40, 000 × g, and enriched in the iodixanol gradient fraction of 1.029 g/ml to 1.056 g/ml (Rutter and Innes 2017), supporting TET8 positive EVs and PEN1 positive EVs are two different sub-populations with different density. Further study is required to determine the density of other EV subtype, such as Exo70E2 positive EVs, by its marker lines or the specific antibodies.

However, density gradient centrifugation has some disadvantages, such as

complex, laborious, time-consuming (up to 2 days). In addition, the other limit of density gradient centrifugation is it difficult to separate different subtypes of EVs with similar densities. Immunoaffinity isolation is the most promise for the separation of the specific subtype of EVs from other subtypes of EVs (Thery et al. 2006; Kowal et al. 2016; Jeppesen et al. 2019; He et al. 2021). Coisolation of nonvesicular contaminants (proteins or RNAs from cytoplasm) and other unwanted vesicles, can be prevented by the highly specific affinity interactions that occur between an antigen and an antibody. The antigens ideally are exosome biomarkers, that are highly concentrated on the exosome membrane, including MHC antigens and tetraspanins proteins (Kowal et al. 2016; Jeppesen et al. 2019). In plant, we showed TET8-positive EVs can be successfully isolated from P100 fraction by the antibody that specifically recognizes the EC2 domain of TET8. Although PEN1 enriched in plant EV membrane, it is not clear whether PEN1 can be used as antigen for immunoaffinity isolation of PEN1 positive EVs. So far, in animal system, there is no report that syntaxin protein can be used to selectively identify and isolate specific subpopulations of EVs. Further studies need to determine whether immunoaffinity isolation can be used for effective separation of PEN1positive EVs.

In this study, we have described the most commonly used EV extraction methods in plants and some comparisons have been made. The current golden standard for plant EV isolation is ultracentrifugation. The density gradient centrifugation technique enables separate different EV subtypes in plant. Since immunoaffinity technique can be done in easy steps, we believed that this method will be widely used in plant EV research in the following years. Together, these findings should serve as a guide to choose and further optimize EVs isolation methods in plant filed for their desired downstream applications.

MATERIALS AND METHODS

Plant materials.

Arabidopsis thaliana ecotype Columbia-0 (*Col-0*) was used in this study. *Arabidopsis* marker lines $TET8_{pro}$*::TET8-GFP* (Cai et al. 2018; He et al. 2021) and

*TET8-GFP/mCherry-PEN*1 double-fluorescence lines (Cai et al. 2018; He et al. 2021), were used as described previously. *Arabidopsis* seeds were grown in soil side-by side at 22 °C for 4 weeks under short-day periods (12 h of light followed by 12 h of darkness).

Collecting the apoplastic washing fluid from *Arabidopsis* leaves.

Collecting the apoplastic washing fluid from *Arabidopsis* leaves was modified from previously studies (O'Leary et al. 2014; Madsen et al. 2016). A typical experiment for EV isolation requires ~100 plants for each genotype/treatment. Distinct proximal (petiole) part of leaves was removed by using scissors, and the distal (blade) zones of leaves were collected. After recording the biomass, leaves were washed 3 times with water. The leaves were carefully placed in 200 ml syringe and gently vacuumed with infiltration buffer (20 mM MES hydrate, 2 mM $CaCl_2$, 0.1 M NaCl, pH 6.0) for 20 seconds. Excess infiltration buffer on leaf surface were removed by clean paper towel and then fixed leaves on small plastic stick. Small plastic stick with leaves were put into a 50 ml conical tube, keeping all leaf opex up, and then centrifuged for 10 min at 4 °C at 900 × g to collect the apoplastic washing fluid.

Isolation of plant EVs by differential ultracentrifugation

Plant EVs were isolated from *Arabidopsis* apoplastic washing fluid. The apoplastic washing fluid was centrifuged for 30 min at 4 °C at 2,000 × g to remove large cell debris and then filtered by a 0.45 μm filter. Next, the supernatants were transferred into new ultracentrifuge tubes and centrifuge for 30 min at 4 °C at 10,000 × g. After the pellet discard, the supernatants (the clean apoplastic washing fluid) were centrifuged for 1 hour at 4 °C at 100,000 × g or 40,000 × g to obtain the P100 EV fraction or P40 EV fraction. To obtain the P100-P40 EV fraction, the supernatants of P40 was centrifuged for 1 hour at 4 °C at 100,000 × g. All pellets were washed in 10 ml of infiltration buffer and finally recentrifuged at the same speed before being resuspended in infiltration buffer for further study.

Iodixanol gradient separation of plant EVs

Discontinuous iodixanol gradients (OptiPrep, STEMCELL) were prepared as described previously protocol with slight modification (Kowal et al. 2016). Working solutions of 10% (v/v), 20% (v/v) and 30% (v/v) idoixanol were made by diluting an aqueous 60% OptiPrep stock solution in infiltration buffer (20 mM MES hydrate, 2 mM $CaCl_2$, 0.1 M NaCl, pH 6.0). The gradient was formed by successively layering 4.8 mL of 30% solution, 2.1 mL of 20% solution, and 2 mL of 10% solution in 13PA tube (himac) from bottom to top. About 0.4 mL of EVs resuspended in infiltration buffer was layered on top of the gradient. The tube was centrifuged for 100,000 × g for 17 h at 4°C (P40ST, CP80NX, himac). After stopping the centrifuge without breaks, 6 fractions of 1.4 ml were collected from top of the tube. These fractions were each brought up to 12 ml with infiltration buffer and centrifuged at 100,000g for 60 min at 4°C to obtain pellet in each fraction.

Electron microscope analysis of plant EVs

Sample preparation of EVs for TEM observation referred to Maroto *et al*.(Maroto et al. 2017). 10 μl of EVs suspension in infiltration buffer was deposited on 3.0 mm copper Formvar-carbon-coated electron microscopy grids (TED PELLA), and then Sample were wicked off using filter paper, and the grids were negatively stained with 10 μl of 1% uranyl acetate. The grids were allowed to air dry and imaged at 100 KV using Transmission Electron Microscope (JEM-1400plus, JEOL). EV size was assessed with Image J software.

Immunoaffinity capture of plant EVs

Immunoaffinity capture of plant EVs were followed as described previously (He et al. 2021). Briefly, Antibodies for immunoaffinity capture, Rabbit polyclonal anti-AtTET8 (Homemade) and normal rabbit immunoglobulin G (Thermo Fisher), were coated with protein A beads in IP buffer (20 mM MES hydrate, 2 mM $CaCl_2$, 0.1 M NaCl, pH 7.5). Beads were then washed 3 times with IP buffer (containing 0.3% BSA), and resuspended in the same buffer, to which P100 fraction was added, followed by overnight incubation at 4 °C with rotation. Bead-bound EVs were collected and washed by IP buffer for further analysis.

Confocal microscopy analyses of plant EVs

For visualization of EV-associated GFP-fluorescence and mcherry-fluorescence, EV pellets or EV coated beads were suspended in infiltration buffer were examined using a 40x water immersion or dip-in lens mounted on a Confocal Laser Scanning Microscope equipped with an argon/krypton laser (Leica TCS SP5).

ACKNOWLEDGEMENTS

Work in the Q.C. laboratory was supported by grants from the National Natural Science Foundation of China (32070288), and supported by Hubei Hongshan Laboratory. Work in the H.J. laboratory was supported by grants from xx.

CONFLICT OF INTEREST

The authors declare no conflict of interest

AUTHOR CONTRIBUTIONS

H.J. and Q.C. designed the experiments. Y.H. and S.W. performed the experiments. Y.H. and Q.C. analyzed the data. Q.C. and H.J. wrote the manuscript. All authors read and approved of its content.

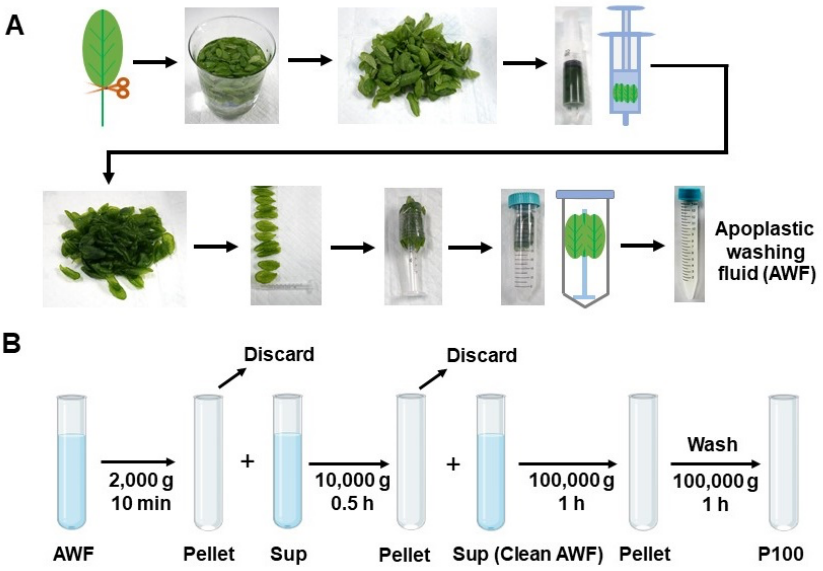

Figure 1. Schematic representation of the plant EV isolation workflow. (A) Images show the various steps in apoplastic washing fluid isolation of *Arabidopsis* (detached leaves protocol, method 1 in Figure 2). Distinct proximal (petiole) part of leaves was removed by using scissors, and the distal (blade) zones of leaves were collected. The leaves were placed in syringe and gently vacuumed with infiltration buffer. Syringe with taped leaves was placed into a 50 ml conical tube, and then centrifuged at 900 × g to collect the apoplastic washing fluid. (B) Scheme of EV isolation by differential ultracentrifugation from apoplastic washing fluid of *Arabidopsis*. The clean apoplastic washing fluid) were centrifuged at 100,000 × g to obtain the P100 EV fraction. Sup, Supernatant. AWF, apoplastic washing fluid.

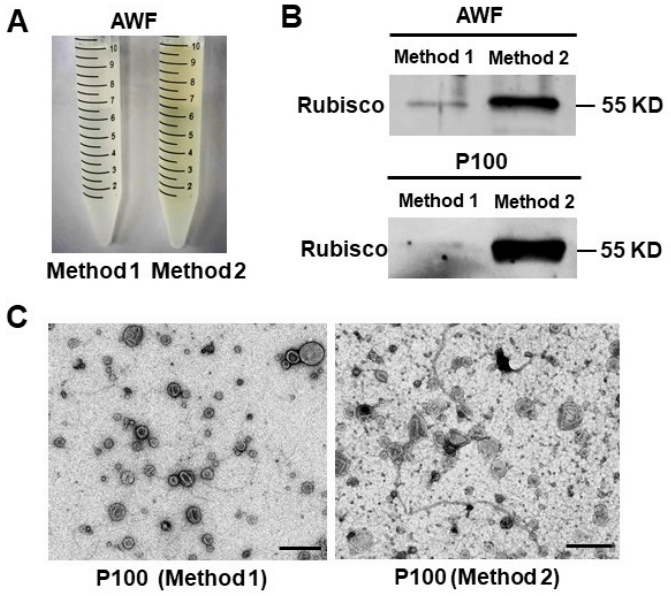

Figure 2. The detached leaves protocol (Method 1) is better for apoplastic washing fluid isolation than whole plant protocol (Method 2) in *Arabidopsis*. (A) Compare the color of apoplastic washing fluid isolated by Method 1 and Method 2. (B) Rubisco protein was detected in both apoplastic washing fluids and their P100 EV fraction by western blot. (C) Representative transmission electron microscopy (TEM) images of P100 fraction isolated from AWF collected by Method 1 and Method 2. Scale bars, 500 nm.

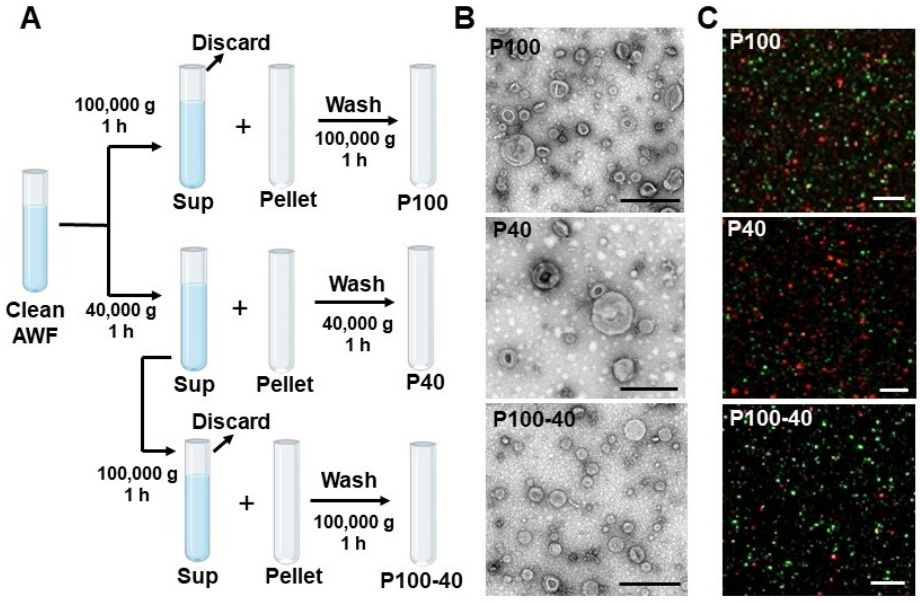

Figure 3. Centrifuged at 100,000 × g enriches plant EVs much more efficiently than

40,000 × g. (A) Scheme of EV isolation by differential ultracentrifugation from apoplastic washing fluid of *Arabidopsis*. EVs isolated from clean apoplastic washing fluid (isolated by Method 1) by ultracentrifugation at 40,000 × g (P40 fraction) and 100,000 × g (P100 fraction) for 1 hour. For the P100-40 fraction, the supernatant of P40 fraction was centrifuged at 100,000 ×g for 1 hour. (B) Representative transmission electron microscopy (TEM) images of P40 fraction, P100 fraction and P100-40 fraction isolated from *B. cinerea*-infected wild-type *Arabidopsis*. For the P100-40 fraction, the supernatant of P40 fraction was centrifuged at 100,000×g for 1 hour. Scale bars, 500 nm. (C) Confocal microscopy of EV fractions isolated from *B. cinerea*-infected *TET8-GFP/mCherry-PEN1* double-fluorescence plants. Scale bars, 5 μm.

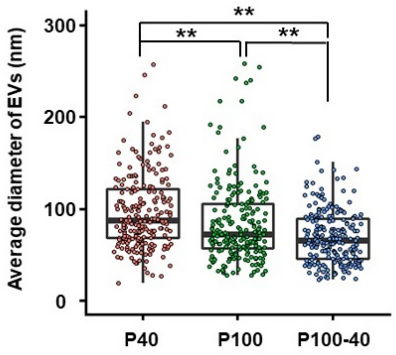

Figure 4. Histograms for the size distribution of EVs in P40 (n = 226 particles analysed, mean = 97.8 nm), P100 (n = 222 particles analysed, mean = 84.5 nm) and P100-40 (n = 232 particles analysed, mean = 69.5 nm) fractions from TEM images. The statistical analysis was performed using ANOVA Dunnett's multiple comparisons test. Each open circles represents a single EV values. **P < 0.01.

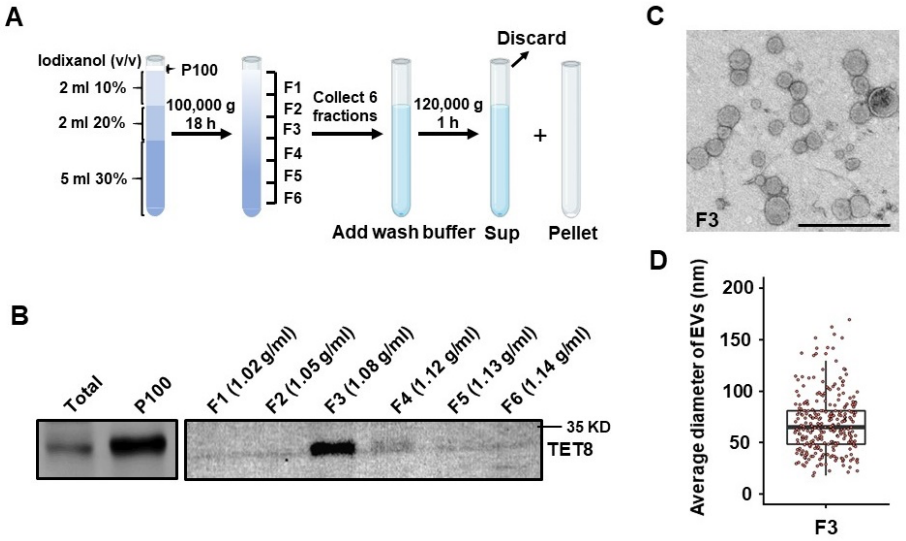

Figure 5. Isolated EVs (P100 fraction) can be further separated by iodixanol gradients centrifugation. (A) P100 fraction obtained after 100,000 × g centrifugations were allowed to float into an overlayed iodixanol gradient by top loading. (B) Six fractions were collected and analyzed by western blot, showing the TET8-positive EV enriched in a single fraction (F3). (C) Representative TEM images of F3 fraction in (B). Scale bars, 500 nm. (D) Histograms for the size distribution of EVs in F3 fraction in (B) (n = 284 particles analysed, mean = of 68.9 nm). Each open circles represents a single EV values.

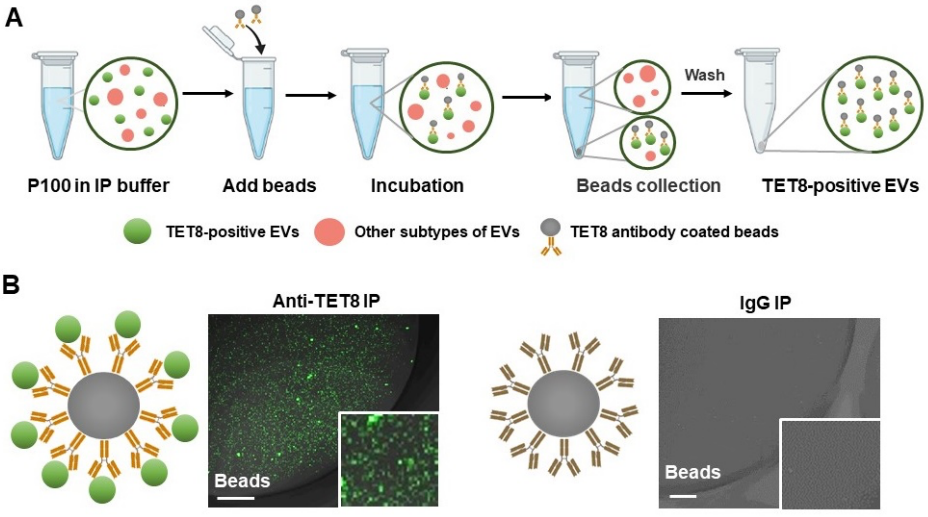

Figure 6. Immunoaffinity isolation is the most advanced method for the purification of

specific subclass of EVs in plant. (A) Scheme of P100 fraction subjected to parallel immuno-isolation with beads coupled to irrelevant Rabbit IgG, or antibodies against TET8. (B) Confocal microscopy of TET8-positive EVs pulled-down by TET8-specific antibody-linked beads. IgG was used as a negative control. Scale bars, 10 um.

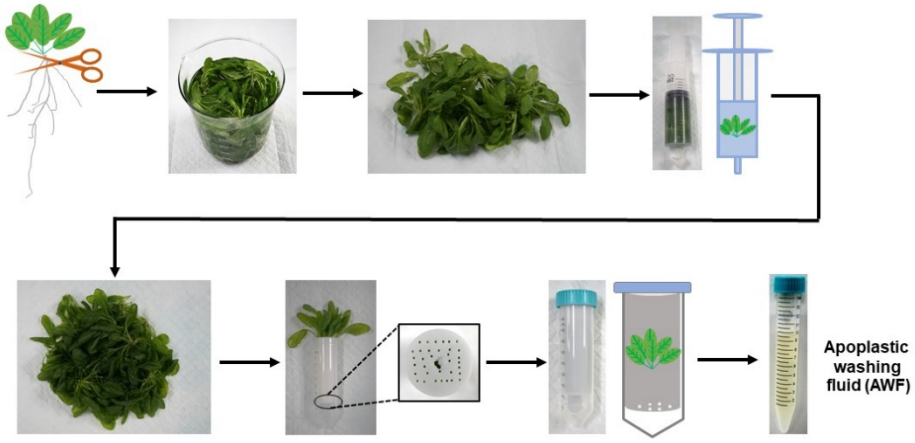

Figure S1. Images show the various steps in apoplastic washing fluid isolation of *Arabidopsis* (Whole rosettes protocol, Method 2 in figure 2). Whole rosettes were harvested at root by using scissors. The rosettes were placed in syringe and gently vacuumed with infiltration buffer, and then placed root down into 30 ml tube with. Next, 30 ml tube was put into 50 ml conical tube, and then centrifuged at 900 × g to collect the apoplastic washing fluid.

REFERENCES

Akers JC, Gonda D, Kim R, Carter BS, Chen CC (2013) Biogenesis of extracellular vesicles (EV): exosomes, microvesicles, retrovirus-like vesicles, and apoptotic bodies. *Journal of neuro-oncology* **113**, 1-11.

An Q, Ehlers K, Kogel KH, van Bel AJ, Huckelhoven R (2006a) Multivesicular compartments proliferate in susceptible and resistant MLA12-barley leaves in response to infection by the biotrophic powdery mildew fungus. *New Phytol* **172**, 563-576.

An Q, Huckelhoven R, Kogel KH, van Bel AJ (2006b) Multivesicular bodies participate in a cell wall-associated defence response in barley leaves attacked by the pathogenic powdery mildew fungus. *Cellular microbiology* **8**, 1009-1019.

An Q, van Bel AJ, Huckelhoven R (2007) Do plant cells secrete exosomes derived from multivesicular bodies? *Plant Signal Behav* **2**, 4-7.

Andreu Z, Yanez-Mo M (2014) Tetraspanins in extracellular vesicle formation and function. *Frontiers in immunology* **5**, 442.

Baldrich P, Rutter BD, Zand Karimi H, Podicheti R, Meyers BC, Innes RW (2019) Plant Extracellular Vesicles Contain Diverse Small RNA Species and Are Enriched in 10 to 17 Nucleotide "Tiny" RNAs. *Plant Cell*.

Bozkurt TO, Belhaj K, Dagdas YF, Chaparro-Garcia A, Wu C, Cano LM, Kamoun S (2014) Rerouting of Plant Late Endocytic Trafficking Toward a Pathogen Interface. *Traffic*.

Cai Q, He B, Jin H (2019a) A safe ride in extracellular vesicles - small RNA trafficking between plant hosts and pathogens. *Curr Opin Plant Biol* **52**, 140-148.

Cai Q, He B, Wang S, Fletcher S, Niu D, Mitter N, Birch PRJ, Jin H (2021) Message in a Bubble: Shuttling Small RNAs and Proteins Between Cells and Interacting Organisms Using Extracellular Vesicles. *Annu Rev Plant Biol* **72**, 497-524.

Cai Q, He B, Weiberg A, Buck AH, Jin H (2019b) Small RNAs and extracellular vesicles: New mechanisms of cross-species communication and innovative tools for disease control. *PLoS Pathog* **15**, e1008090.

Cai Q, Qiao L, Wang M, He B, Lin FM, Palmquist J, Huang SD, Jin H (2018) Plants send small RNAs in extracellular vesicles to fungal pathogen to silence virulence genes. *Science* **360**, 1126-1129.

Colombo M, Raposo G, Thery C (2014) Biogenesis, secretion, and intercellular interactions of exosomes and other extracellular vesicles. *Annu Rev Cell Dev Biol* **30**, 255-289.

Crescitelli R, Lasser C, Szabo TG, Kittel A, Eldh M, Dianzani I, Buzas EI, Lotvall J (2013) Distinct RNA profiles in subpopulations of extracellular vesicles: apoptotic bodies, microvesicles and exosomes. *Journal of extracellular vesicles* **2**.

Ding Y, Wang J, Chun Lai JH, Ling Chan VH, Wang X, Cai Y, Tan X, Bao Y, Xia J, Robinson DG, Jiang L (2014) Exo70E2 is essential for exocyst subunit recruitment and EXPO formation in both plants and animals. *Mol Biol Cell* **25**, 412-426.

Halperin W, Jensen WA (1967) Ultrastructural Changes during Growth and Embryogenesis in Carrot Cell Cultures. *Journal of ultrastructure research* **18**, 428-&.

Hatsugai N, Iwasaki S, Tamura K, Kondo M, Fuji K, Ogasawara K, Nishimura M, Hara-Nishimura I (2009) A novel membrane fusion-mediated plant immunity against bacterial

pathogens. *Genes Dev* **23**, 2496-2506.

He BY, Cai Q, Qiao LL, Huang CY, Wang SM, Miao WL, Ha T, Wang YS, Jin HL (2021) RNA-binding proteins contribute to small RNA loading in plant extracellular vesicles. *Nature plants*.

Hou Y, Zhai Y, Feng L, Karimi HZ, Rutter BD, Zeng L, Choi DS, Zhang B, Gu W, Chen X, Ye W, Innes RW, Zhai J, Ma W (2019) A Phytophthora Effector Suppresses Trans-Kingdom RNAi to Promote Disease Susceptibility. *Cell Host Microbe* **25**, 153-165 e155.

Huang CY, Wang H, Hu P, Hamby R, Jin H (2019) Small RNAs - Big Players in Plant-Microbe Interactions. *Cell Host Microbe* **26**, 173-182.

Iliev D, Strandskog G, Nepal A, Aspar A, Olsen R, Jorgensen J, Wolfson D, Ahluwalia BS, Handzhiyski J, Mironova R (2018) Stimulation of exosome release by extracellular DNA is conserved across multiple cell types. *FEBS J* **285**, 3114-3133.

Jeppesen DK, Fenix AM, Franklin JL, Higginbotham JN, Zhang Q, Zimmerman LJ, Liebler DC, Ping J, Liu Q, Evans R, Fissell WH, Patton JG, Rome LH, Burnette DT, Coffey RJ (2019) Reassessment of Exosome Composition. *Cell* **177**, 428-445 e418.

Jung MK, Mun JY (2018) Sample Preparation and Imaging of Exosomes by Transmission Electron Microscopy. *J Vis Exp*.

Kameli N, Dragojlovic-Kerkache A, Savelkoul P, Stassen FR (2021) Plant-Derived Extracellular Vesicles: Current Findings, Challenges, and Future Applications. *Membranes* **11**.

Kimura M, Anzai H, Yamaguchi I (2001) Microbial toxins in plant-pathogen interactions: Biosynthesis, resistance mechanisms, and significance. *The Journal of general and applied microbiology* **47**, 149-160.

Knip M, Constantin ME, Thordal-Christensen H (2014) Trans-kingdom Cross-Talk: Small RNAs on the Move. *Plos Genetics* **10**.

Konoshenko MY, Lekchnov EA, Vlassov AV, Laktionov PP (2018) Isolation of Extracellular Vesicles: General Methodologies and Latest Trends. *BioMed research international* **2018**, 8545347.

Kowal J, Arras G, Colombo M, Jouve M, Morath JP, Primdal-Bengtson B, Dingli F, Loew D, Tkach M, Thery C (2016) Proteomic comparison defines novel markers to characterize heterogeneous populations of extracellular vesicle subtypes. *Proc Natl Acad Sci U S A* **113**, E968-977.

Liu L, Chen X (2018) Intercellular and systemic trafficking of RNAs in plants. *Nature plants* **4**, 869-878.

Liu Y, Wu S, Koo Y, Yang A, Dai Y, Khant H, Osman SR, Chowdhury M, Wei H, Li Y, Court K, Hwang E, Wen Y, Dasari SK, Nguyen M, Tang EC, Chehab EW, de Val N, Braam J, Sood AK (2020) Characterization of and isolation methods for plant leaf nanovesicles and small extracellular vesicles. *Nanomedicine* **29**, 102271.

Madsen SR, Nour-Eldin HH, Halkier BA (2016) Collection of Apoplastic Fluids from Arabidopsis thaliana Leaves. *Methods Mol Biol* **1405**, 35-42.

Mahlapuu M, Hakansson J, Ringstad L, Bjorn C (2016) Antimicrobial Peptides: An Emerging Category of Therapeutic Agents. *Frontiers in cellular and infection microbiology* **6**, 194.

Maroto R, Zhao Y, Jamaluddin M, Popov VL, Wang H, Kalubowilage M, Zhang Y, Luisi J, Sun H, Culbertson CT, Bossmann SH, Motamedi M, Brasier AR (2017) Effects of storage temperature on airway exosome integrity for diagnostic and functional analyses. *Journal of extracellular vesicles* **6**, 1359478.

Mathieu M, Martin-Jaular L, Lavieu G, Thery C (2019) Specificities of secretion and uptake of

exosomes and other extracellular vesicles for cell-to-cell communication. *Nature cell biology* **21**, 9-17.

Mathivanan S, Fahner CJ, Reid GE, Simpson RJ (2012) ExoCarta 2012: database of exosomal proteins, RNA and lipids. *Nucleic Acids Res* **40**, D1241-1244.

Movahed N, Cabanillas DG, Wan J, Vali H, Laliberte JF, Zheng HQ (2019) Turnip Mosaic Virus Components Are Released into the Extracellular Space by Vesicles in Infected Leaves. *Plant Physiology* **180**, 1375-1388.

Mu JY, Zhuang XY, Wang QL, Jiang H, Deng ZB, Wang BM, Zhang LF, Kakar S, Jun Y, Miller D, Zhang HG (2014) Interspecies communication between plant and mouse gut host cells through edible plant derived exosome-like nanoparticles. *Molecular nutrition & food research* **58**, 1561-1573.

Musante L, Saraswat M, Ravida A, Byrne B, Holthofer H (2013) Recovery of urinary nanovesicles from ultracentrifugation supernatants. *Nephrology, dialysis, transplantation : official publication of the European Dialysis and Transplant Association - European Renal Association* **28**, 1425-1433.

Nielsen ME, Feechan A, Bohlenius H, Ueda T, Thordal-Christensen H (2012) Arabidopsis ARF-GTP exchange factor, GNOM, mediates transport required for innate immunity and focal accumulation of syntaxin PEN1. *Proc Natl Acad Sci U S A* **109**, 11443-11448.

O'Leary BM, Rico A, McCraw S, Fones HN, Preston GM (2014) The infiltration-centrifugation technique for extraction of apoplastic fluid from plant leaves using Phaseolus vulgaris as an example. *J Vis Exp*.

Prado N, Alche JD, Casado-Vela J, Mas S, Villalba M, Rodriguez R, Batanero E (2014) Nanovesicles Are Secreted during Pollen Germination and Pollen Tube Growth: A Possible Role in Fertilization. *Molecular Plant* **7**, 573-577.

Prado N, De Linares C, Sanz ML, Gamboa P, Villalba M, Rodriguez R, Batanero E (2015) Pollensomes as Natural Vehicles for Pollen Allergens. *Journal of Immunology* **195**, 445-449.

Regente M, Corti-Monzon G, Maldonado AM, Pinedo M, Jorrin J, de la Canal L (2009) Vesicular fractions of sunflower apoplastic fluids are associated with potential exosome marker proteins. *FEBS Lett* **583**, 3363-3366.

Regente M, Pinedo M, San Clemente H, Balliau T, Jamet E, de la Canal L (2017) Plant extracellular vesicles are incorporated by a fungal pathogen and inhibit its growth. *J Exp Bot* **68**, 5485-5495.

Roth R, Hillmer S, Funaya C, Chiapello M, Schumacher K, Lo Presti L, Kahmann R, Paszkowski U (2019) Arbuscular cell invasion coincides with extracellular vesicles and membrane tubules. *Nature plants* **5**, 204-211.

Rutter BD, Innes RW (2017) Extracellular Vesicles Isolated from the Leaf Apoplast Carry Stress-Response Proteins. *Plant Physiol* **173**, 728-741.

Sanmartin M, Ordonez A, Sohn EJ, Robert S, Sanchez-Serrano JJ, Surpin MA, Raikhel NV, Rojo E (2007) Divergent functions of VTI12 and VTI11 in trafficking to storage and lytic vacuoles in Arabidopsis. *Proc Natl Acad Sci U S A* **104**, 3645-3650.

Teng Y, Ren Y, Sayed M, Hu X, Lei C, Kumar A, Hutchins E, Mu JY, Deng ZB, Luo C, Sundaram K, Sriwastva MK, Zhang LF, Hsieh M, Reiman R, Haribabu B, Yan J, Jala VR, Miller DM, Van Keuren-Jensen K, Merchant ML, McClain CJ, Park JW, Egilmez NK, Zhang HG (2018) Plant-Derived Exosomal MicroRNAs Shape the Gut Microbiota. *Cell Host & Microbe* **24**, 637-+.

Thery C, Amigorena S, Raposo G, Clayton A (2006) Isolation and characterization of exosomes

from cell culture supernatants and biological fluids. *Current protocols in cell biology / editorial board, Juan S. Bonifacino ... [et al.]* **Chapter 3**, Unit 3 22.

Toruno TY, Stergiopoulos I, Coaker G (2016) Plant-Pathogen Effectors: Cellular Probes Interfering with Plant Defenses in Spatial and Temporal Manners. *Annual Review Of Phytopathology, Vol 54* **54**, 419-441.

van Niel G, D'Angelo G, Raposo G (2018) Shedding light on the cell biology of extracellular vesicles. *Nat Rev Mol Cell Bio* **19**, 213-228.

Wang D, Weaver ND, Kesarwani M, Dong XN (2005) Induction of protein secretory pathway is required for systemic acquired resistance. *Science* **308**, 1036-1040.

Wang J, Ding Y, Wang J, Hillmer S, Miao Y, Lo SW, Wang X, Robinson DG, Jiang L (2010) EXPO, an exocyst-positive organelle distinct from multivesicular endosomes and autophagosomes, mediates cytosol to cell wall exocytosis in Arabidopsis and tobacco cells. *Plant Cell* **22**, 4009-4030.

Wang QL, Zhuang XY, Mu JY, Deng ZB, Jiang H, Xiang XY, Wang BM, Yan J, Miller D, Zhang HG (2013) Delivery of therapeutic agents by nanoparticles made of grapefruit-derived lipids. *Nature communications* **4**.

Willms E, Cabanas C, Mager I, Wood MJA, Vader P (2018) Extracellular Vesicle Heterogeneity: Subpopulations, Isolation Techniques, and Diverse Functions in Cancer Progression. *Frontiers in immunology* **9**, 738.

Wubbolts R, Leckie RS, Veenhuizen PT, Schwarzmann G, Mobius W, Hoernschemeyer J, Slot JW, Geuze HJ, Stoorvogel W (2003) Proteomic and biochemical analyses of human B cell-derived exosomes. Potential implications for their function and multivesicular body formation. *J Biol Chem* **278**, 10963-10972.

Zhang HG, Cao P, Teng Y, Hu X, Wang Q, Yeri AS, Zhuang X, Samykutty A, Mu J, Deng ZB, Zhang L, Mobley JA, Yan J, Van Keuren-Jensen K, Miller D (2016a) Isolation, identification, and characterization of novel nanovesicles. *Oncotarget* **7**, 41346-41362.

Zhang S, Sun L, Kragler F (2009) The phloem-delivered RNA pool contains small noncoding RNAs and interferes with translation. *Plant Physiol* **150**, 378-387.

Zhang T, Zhao YL, Zhao JH, Wang S, Jin Y, Chen ZQ, Fang YY, Hua CL, Ding SW, Guo HS (2016b) Cotton plants export microRNAs to inhibit virulence gene expression in a fungal pathogen. *Nature plants* **2**, 16153.